DNA Compaction by the Nuclear Factor-Y

Rosalinda F. Guerra,* Laura Imperadori,* Roberto Mantovani,[†] David D. Dunlap,[‡] and Laura Finzi[§]

Departments of *Biology and [†]Biotechnological and Biomolecular Sciences, University of Milan, Milan Italy;
and Departments of [‡]Cell Biology and [§]Physics, Emory University, Atlanta, Georgia

ABSTRACT   The nuclear factor-Y (NF-Y), a trimeric, CCAAT-binding transcriptional activator with histone-like subunits, was until recently considered a prototypical promoter transcription factor. However, recent in vivo chromatin immunoprecipitation assays associated with microarray methodologies (chromatin immunoprecipitation on chip experiments) have indicated that a large portion of target sites (40%–50%) are located outside of core promoters. We applied the tethered particle motion technique to the major histocompatibility complex class II enhancer-promoter region to characterize i), the progressive compaction of DNA due to increasing concentrations of NF-Y, ii), the role of specific subunits and domains of NF-Y in the process, and iii), the interplay between NF-Y and the regulatory factor-X, which cooperatively binds to the X-box adjacent to the CCAAT box. Our study shows that NF-Y has histone-like activity, since it binds DNA nonspecifically with high affinity to compact it. This activity, which depends on the presence of all trimer subunits and of their glutamine-rich domains, seems to be attenuated by the transcriptional cofactor regulatory factor-X. Most importantly NF-Y-induced DNA compaction may facilitate promoter-enhancer interactions, which are known to be critical for expression regulation.

INTRODUCTION

The eukaryotic transcription factor nuclear factor-Y (NF-Y) was originally identified as a mouse protein recognizing the Y box in the major histocompatibility complex of class II (MHCII) promoters (1). This factor specifically recognizes the regulatory CCAAT element found in either orientation in the proximal and distal enhancer regions of many genes (2). For this reason, NF-Y is also called CCAAT binding factor. The CCAAT box is a widespread regulatory sequence found in promoters and enhancers of several genes. The functional importance of the CCAAT box has been well established in different systems. Analysis of 1031 promoters established that ~30% contain such an element, preferentially located in the −60/−100 region with respect to the transcription initiation site (3). In general, the position and orientation as well as the nucleotides flanking the central CCAAT pentanucleotide are extremely well conserved within the same gene across species. The CCAAT box is usually found in the vicinity of the other promoter elements, and in many cases the relative distance is critical for proper transcription. Indeed, CCAAT box bending and/or direct protein-protein interactions have often been reported (2).

A number of genetic and biochemical experiments established unambiguously that NF-Y is the CCAAT activator. NF-Y is a heterotrimeric complex composed of the NF-YA, NF-YB, and NF-YC subunits, which are all required for CCAAT binding. Each subunit contains a core region that has been highly conserved throughout evolution and that is sufficient for subunit interactions and CCAAT binding, whereas the flanking regions, which include the activation domains, are much less conserved (Fig. 1 *B*). NF-YC and NF-YB core regions are homologous in sequence to histones H2A and H2B, respectively, and are required for heterodimerization, a prerequisite for NF-YA association and CCAAT binding (4). The structure of the complex between the conserved regions of human NF-YB and NF-YC was studied by x-ray crystallography. The structure was refined at 1.6-Å resolution and shows that the proteins interact through histone fold motifs in a head-to-tail fashion. Based on this, it was suggested that the dimer interacts directly and nonspecifically with DNA, similarly to H2A/H2B, and that the NF-YA subunit stabilizes the complex and enables sequence-specific binding (5). The core domain of NF-YA is less than 60 amino acids long and is sufficient for DNA binding when complexed with NF-YC/NF-YB. Several studies have established two distinct parts of the NF-YA core domain: an N-terminal domain responsible for NF-YC/NF-YB binding and a C-terminal domain implicated in specific recognition of the CCAAT sequence (6).

Once the trimeric complex is formed, it binds DNA with very high specificity and affinity. Indeed, the K_d is between 10^{-10} and 10^{-11} M, among the highest of all transcriptional factors (7,8). Specific recognition of the bases by the protein seems to involve both minor and major groove interactions, and circular permutation assays indicated that, upon binding, the DNA is bent by ~60°–80° (9,10). It is thought that such bending might be necessary to give the exact orientation to other transcriptional factors, such as the regulatory factor-X (RFX), for transcriptional activation. Until recently, NF-Y binding sites far from the promoter were thought uncommon. However, chromatin immunoprecipitation on chip (ChIP-on-chip) techniques have identified a large number (40% of the total) of genomic loci bound by NF-Y in vivo that are distant from the promoter, either in introns or at extremities (either
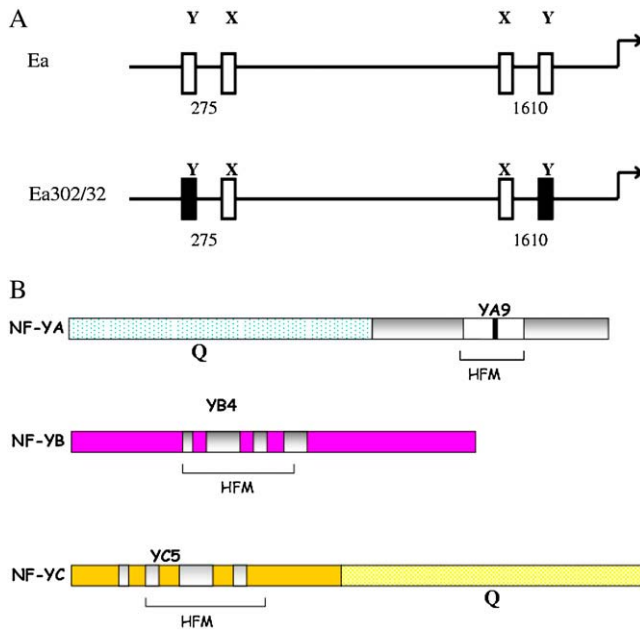
FIGURE 1 Schematic representation of the fragments of DNA and the proteins used. (*A*) *Ea* represents the fragment of DNA where the Y elements are the two CCAAT boxes recognized by NF-Y and the X elements are specific sites for RFX binding, and *Ea302/32* represents a similar fragment containing mutated CCAAT boxes, which prevent NF-Y binding. (*B*) Schematic representation of the three subunits constituting the heterotrimeric complex of NF-Y. HFM stands for histone fold motif; YA9, YB4, and YC5 are core regions highly conserved, and Q indicates a Q-rich domain (*bottom*).

3′ or 5′) of genes (11). From chromatin immunoprecipitation (ChIP) experiments, it is clear that in vivo association of NF-Y to promoters and enhancers is essential for gene function. Some of the transcriptional loci in which the interplay between these sites have been shown to be functionally relevant are the tissue-specific MHCII genes, in which the activity of both core promoters and enhancers 1–1.5 Kb upstream, a combination present in all genes of the family, are controlled by the cooperative binding of RFX and NF-Y (12).

Given these premises, we became interested in the possible interaction between two distantly bound NF-Y molecules. These could interact via the formation of a DNA loop, which would bring the enhancer and promoter CCAAT boxes into proximity with one another or via more complex architectural changes mediated by the histone-like properties of NF-Y. Either kind of conformational change in DNA may indicate additional regulatory roles for the protein. Therefore, we used the TPM technique to study the effect of increasing NF-Y concentrations on DNA molecules. This technique allows monitoring of the formation and breakdown of conformational changes induced by proteins on DNA. The amplitude of the Brownian motion of a mechanical probe, such as a microsphere, tethered by a single DNA molecule to the glass surface of a microscope flow chamber is monitored in real time and reflects changes in the DNA length.

TPM offers certain advantages over static imaging techniques such as electron microscopy and atomic force microscopy, in that sample preparation does not require electron-dense staining or adsorption of the protein to surfaces, which may introduce artifacts. TPM has previously been used to study DNA loop formation and breakdown induced by prokaryotic transcriptional factors (13,14) and, thus, to obtain insight into the regulatory aspects of such proteins and their partners. This study represents the first use of single-molecule microscopy to characterize the interaction of a eukaryotic (not prokaryotic), non-ATP-dependent transcriptional factor with DNA. Here, we analyzed the effect of different concentrations of NF-Y and RFX on DNA architecture and how RFX modulates these changes. We report on the DNA compaction promoted by NF-Y, which supports the idea that NF-Y binding is not restricted to promoters and may mediate promoter/ enhancer cross talk.

MATERIALS AND METHODS

DNA and protein preparation

DNA constructs

The 1851-bp-long DNA fragment, containing two distant CCAAT boxes, was obtained from enzymatic digestion of plasmid pS3 (15) with the restriction enzymes Sal1 and *Hin*dIII (New England BioLabs, Hertfordshire, UK). The enzymatic digestion product was isolated electrophoretically and purified (Qiagen purification kit, Qiagen, Hilden, Germany). The ends of the fragment were labeled with digoxigenin (dUTP-dig, Roche, Mannheim, Germany) and biotin (dUTP-bio, Roche) using the Klenow fragment of the polymerase I from *Escherichia coli*. A second round of purification was then performed.

The same protocol was followed for a similar fragment containing mutant CCAAT boxes, which do not bind NF-Y. In both constructs the Y and Y′ boxes were 300 bp and 340 bp, respectively, from the ends. Such distances are appropriate to reveal possible conformational changes in the DNA due to the interaction between the two CCAAT boxes.

RFX and NF-Y proteins

Wild-type and mutant proteins were obtained as described previously: NF-Y (10), RFX. (16).

Tethered particle microscopy

The tethered particle motion (TPM) technique or tethered particle microscopy, as it is more recently being called, consists of observing through an optical microscope the Brownian motion of a small particle (bead) tethered to the glass surface of a microscope flow chamber by a single molecule of nucleic acid (Fig. 2). The tether is invisible, but the range of Brownian motion of the bead depends on its tether length and, thus, can be used to infer the length of nucleic acid tethers. Furthermore, temporal changes in the Brownian motion can be used to monitor changes in tether length over time (17).

Preparation of microscope flow chambers

The proteins were diluted in the following buffer: 200 mM Tris-HCl, pH 7.5, 0.2 M KCl, 0.1 M EDTA, 0.1 M dithiothreitol (DTT), 5% dimethylsulfoxide (DMSO), α-casein (Sigma, Schnelldorf, Germany) 10 mg/ml. And the

microspheres (400 nm in diameter) and the DNA were diluted in 200 mM Tris-HCl pH 7.5, 0.2 M KCl, 0.1 M EDTA. The DNA concentration was 4.92×10^{-11} M.

The flow chambers (~20 μl volume) were built by mounting coverslips on microscope slides with double-sided adhesive tape. They were first coated with 40 μg/ml Bio-BSA (Sigma) for 2 h at room temperature. After washing with 800 μl of buffer, supplemented with α-casein, to prevent nonspecific adhesion of DNA to the glass, the chamber was incubated with 50 μg/ml streptavidin (Sigma) for 2 h. After incubation the excess of streptavidin was washed with 800 μl of buffer. The mixture of DNA/ microspheres that had been previously incubated (Antidigoxigenin polysty-rene particles, Indicia, Oullins, France) was inserted in the microchamber and left for 1 h (18), and the unbound DNA and microspheres were washed with 800 μl of buffer. This operation left a final concentration of surface-bound DNA of roughly 10^{-14} M (13). After 30 min of registration, NF-Y was added to the chamber, and the recording of bead motion resumed immediately for other 30 min before the solution was changed to either increase the concentration of NF-Y or add RFX. Each sample condition was recorded for 30 min.

Single-particle tracking experiments

Image acquisition of the tethered microspheres was performed by differential interference contrast microscopy at room temperature. The microscope (DM LB2-100, Leica, Wetzlar, Germany) was equipped with an oil-immersion, 100× objective. Images were recorded with a charge-coupled device camera (JAI CV-M10, Copenhagen, Denmark) at a video rate of 25 frames/s on a videotape recorder (Panasonic NV-HS930, Secaucus, NJ) and digitalized using a real-time acquisition board (IMAQ PCI-1409, National Instruments, Austin, TX). Images were analyzed using in-house software written using Labview (version 6.2) which extracts the position coordinates of the microspheres (x_n, y_n). These were then saved on a hard disk and used to evaluate the root mean-square displacement,

$$\sigma = \sqrt{\frac{\sum_{i=1}^{N}(x_i - \bar{x})^2 + (y_i - \bar{y})^2}{N}}$$

(18) over a time window of 4 s.

RESULTS

To begin, we investigated the effect of increasing concentrations of the NF-Y trimer on the conformation of single DNA molecules containing two CCAAT boxes separated by 1335 bp (Fig. 1 A). The amplitude of the Brownian motion of microspheres tethered to the glass surface of a microscope flow chamber by a single DNA molecule permits direct measurement of the average length of the tethering molecule and reveals protein-mediated conformational changes in the overall DNA length. For this experiment, we used a DNA construct containing the MHCII Ea promoter-enhancer sequences (15), named Ea (Fig. 1 A), and recorded the amplitude of motion of microspheres as a function of time (Fig. 3 A). The figure shows that tether lengths were very stable over time.

The traces in Fig. 3 A depict the movement of one single microsphere bound to a single DNA molecule in the presence of different NF-Y concentrations. Several NF-Y concentrations were tried on the DNA (0.15, 0.3, 0.6, 1.2, 1.8, 3.6, 9 nM), but only those that showed a change in the end-to-end
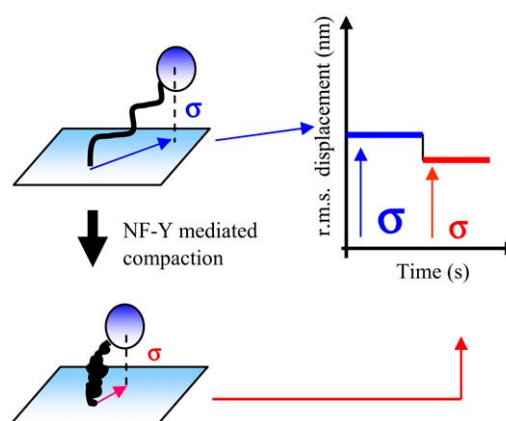

FIGURE 2 Schematic representation of the TPM experimental setup. (*Left*) a submicron-size bead is tethered to the glass surface of a flow microchamber by a single DNA molecule. Addition of NF-Y induces a change in the effective length of the tethering DNA, causing a decrease in the average Brownian motion of the microsphere measured by σ. This difference is visualized as the amplitude of the Brownian motion of the bead as a function of time.

distance of the DNA are reported in the figure. In the absence of NF-Y (*yellow trace*), the movement of the microsphere is larger than in the presence of NF-Y at concentrations $\geq$1.2 nM. Noticeably, NF-Y causes a progressive decrease in the overall length of the DNA molecule and a consequent reduction of the amplitude of motion of the microsphere to a minimum value of 190 nm (*purple trace*) when the concentration of NF-Y reaches 3.6 nM. This compaction effect is schematized in Fig. 3 B, where each point in the graph represents the average value of the points in the trace recorded for each of the microspheres (A, B, etc.) at a given NF-Y concentration. Table 1 summarizes the mean TPM value observed for the different samples of beads in Fig. 3 B with its standard deviation.

For each given experimental condition, all microspheres behaved similarly. Using an experimental calibration curve obtained in the lab (18), we were able to relate each measured root mean-square displacement (σ) to an apparent DNA length. Although the average value of σ obtained in control experiments, 269 nm ± 3 nm, is in agreement with the known length of the DNA template used, the average σ values recorded at 1.2, 1.8, and 3.6 nM NF-Y (240 ± 14, 205 ± 9, 190 ± 8 nm) correspond to apparent DNA lengths of 1380, 1000, and 800 bp, respectively. These values indicate overall compaction of ~26%, 46%, and 57% for those NF-Y concentrations. The absolute degree of compaction is hard to estimate since i) protein binding to DNA can change the flexibility of the double helix in either direction depending on protein characteristics and conditions (19,20), and ii) the effect of NF-Y on DNA elasticity has not yet been characterized.

To understand what domain of the NF-Y trimer may be responsible for DNA compaction, we performed several experiments to compare the compaction induced by incomplete NF-Y proteins (Fig. 4). As in Fig. 3, each point in the
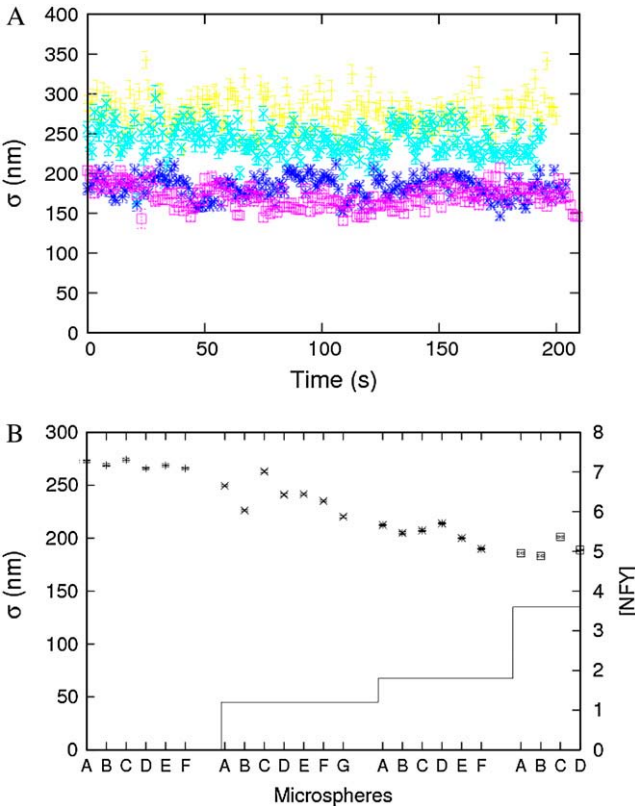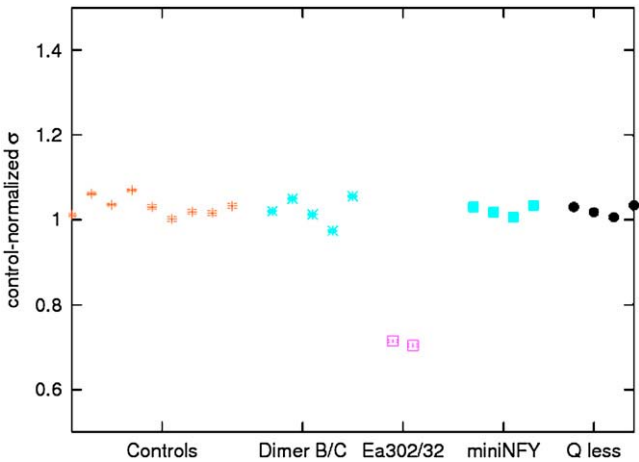
FIGURE 4   Effect of mutant NF-Y proteins and the CCAAT box on compaction. Here, the y axis reports the root mean-square displacement, σ, which is normalized to the value in the absence of NF-Y. The red dots refer to DNA in the absence of NF-Y (controls). Turquoise star points refer to Ea DNA in the presence of dimer NF-YB/C. Purple data represent Ea302/32 DNA in the presence of wild-type NF-Y. Turquoise squares represent Ea in the presence of mini-NF-Y (YA9/NF-YB/C), and black circles describe the interaction between Ea and Q-less (YA9/NF-YB/YC5). In all cases, the concentration of protein was 3.6 nM. Each point represents the average value of the Brownian motion of a microsphere tethered by a single DNA molecule. As in the previous figure, the standard deviation is indicated for each data point although it is often too small to be visible.

FIGURE 3   Effect of the concentration increase of NF-Y on Ea. (*A*) The root mean-square displacement (σ) of the microsphere is plotted versus the time of acquisition. Each color represents the trace relative to a single microsphere bound to DNA. Yellow is the control in the absence of NF-Y; turquoise, blue, and purple are in the presence of 1.2, 1.8, and 3.6 nM NF-Y respectively. (*B*) The average root mean-square displacement is plotted for individual microspheres (A, B, C, . . .). Each point represents the average value of the Brownian motion of one microsphere tethered by a single DNA molecule. The same letter represents the same microsphere in conditions of increasing concentrations of NF-Y. The stepped line at the bottom of (*B*) indicates different concentrations of NF-Y. The standard deviation is often too small to be visible.

graph represents the average value of an entire trace, except that these values have been normalized with respect to the control recorded in the absence of protein. It is clear that the mutant proteins do not cause any compaction. The red points on the left show the average value of the Brownian motion of

microspheres tethered by single Ea DNA molecules in the absence of protein. These values were used in the normalization process. With respect to this reference, the presence of NF-YB/NF-YC dimers (B/C) does not compact DNA, even at 40 nM (*turquoise stars*).

Also shown on the right are the average amplitudes of Brownian motion of microspheres tethered by single Ea DNA molecules in the presence of two other NF-Y mutants: respectively, mini-NF-Y, formed by the B/C dimer together with the YA9 domain of NF-YA (Fig. 1 *B*), and a protein called Q-less, formed by YA9 together with NF-YB and YC5, which is a trimer without Q-rich domains. Neither of these mutants induces DNA compaction at a concentration of 3.6 nM. However 3.6 nM wild-type NF-Y efficiently compacted DNA molecules in which the two CCAAT boxes were mutated (Ea302/32, Fig. 1 *A*) to weaken specific NF-Y binding (*central purple squares*).

Since the transcription factor RFX is important in the transcriptional control of MHCII genes (21), we have also studied its effect on DNA. We first investigated the effect of RFX alone on DNA and, later, that of RFX together with NF-Y. To assess the effect of RFX alone on DNA, we incubated in the flow chamber two different concentrations of the protein and found that the average value of the length of single DNA molecules did not change with increasing RFX concentration (Fig. 5). This is shown by the constant value of the Brownian motion of microspheres tethered by single Ea DNA molecules (A-L) in the absence of RFX and in the

TABLE 1   Average TPM signal and relative standard deviation obtained from the beads reported in Fig. 3 *B* at different NF-Y concentrations

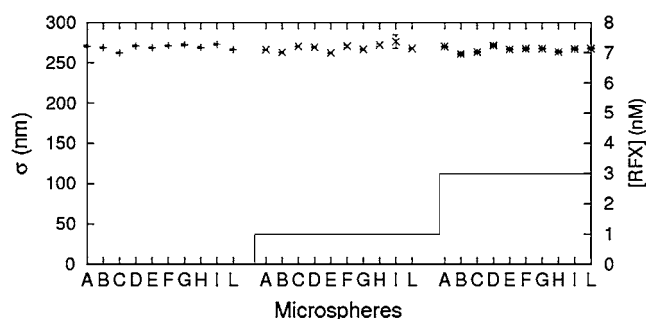| [NF-Y]	Number of beads	Mean σ (nm)	SD (nm)
0	6	269.3	±3
0.6	6	267.8	±4
1.2	6	243	±13
1.8	6	205	±9
3.6	4	190	±8
9	3	180	±12

SD, standard deviation.

FIGURE 5 Effect of RFX on Ea. The average value of the Brownian motion of various microspheres (A–L) each tethered by a single Ea DNA molecule is reported in the presence of various increasing concentrations of RFX. The right-hand side y axis indicates the concentration of RFX in nM $\times$ 10^{-1}. The first 10 points in the graph refer to DNA in control experimental conditions, the following 10 points refer to the same DNA molecules in the presence of RFX 10 nM, and the third group of points refer to the same DNA molecules in the presence of RFX 30 nM. The stepped line at the bottom of the graph indicates the two RFX concentrations used. The standard deviation is indicated for each data point although it is often too small to be visible.

presence of RFX. On the other hand, RFX seems to interfere with the DNA compaction induced by NF-Y. This is shown by a comparative analysis of Figs. 3 B and 6, where RFX was 30 nM (the highest concentration used in the experiment above), along with two different concentrations of NF-Y, 1.2 nM, and 1.8 nM that had shown different levels of DNA compaction. The root mean-square displacement recorded in the presence of 1.2 nM NF-Y increases from 240 ± 14 nm to 251 ± 9 nm if RFX is also added, leading to an overall apparent DNA length of 1680 bp and a compaction of 10% instead of 26%. The root mean-square displacement recorded
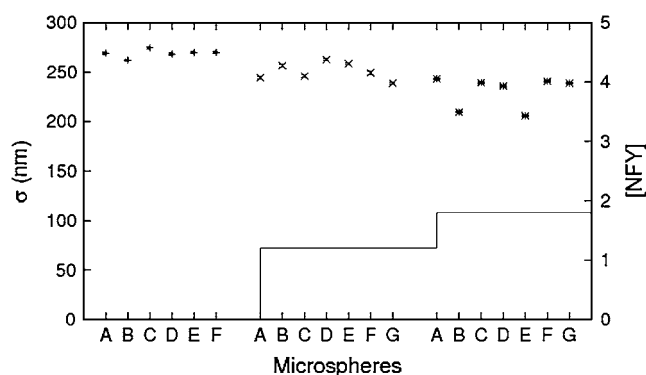

FIGURE 6 Interaction between the RFX/NF-Y complex and Ea. The first six data points represent the average value of the Brownian motion of various microspheres (A–F), each tethered by a single Ea DNA molecule in the absence of protein. The following data points refer to measurements in which the concentration of RFX is maintained constant at 30 nM and the concentrations of NF-Y are varied (1.2 nM, *stars* and 1.8 nM, *squares*). The stepped line at the bottom represents the different concentrations of NF-Y. The standard deviation is indicated for each data point although it is often too small to be visible.

in the presence of 1.8 nM NF-Y increases from 205 ± 9 nm to 231 ± 16 nm if RFX is also added, leading to an overall apparent DNA length of 1340 bp and a compaction of 28% instead of 46%.

DISCUSSION

Recent in vivo ChIP experiments on CpG islands' genomic arrays surprisingly established that a large portion of NF-Y target sites are located away from core promoters in intron, upstream, and downstream regions (11). It is likely that these locations represent enhancers or other regulatory areas. Previously, only a few examples of promoter enhancers combinations on which NF-Y acted were known. One of these was represented by the MHC class II system. A plethora of biochemical, genetic, and ChIP data suggested the fundamental role of NF-Y and of the neighboring X-binding RFX for all MHC class II genes. Mutation analysis in transgenic mice of either promoter or enhancer Y or X box altered physiological expression (1,12). The question is, therefore, how does NF-Y help promoter-enhancer communications?

The TPM technique provides a powerful tool to address this issue. Our data show that although TPM was not sensitive enough to reveal the DNA bending due to a single NF-Y molecule, which is expected to be ~60°/80° (10), it revealed that NF-Y progressively compacts DNA at concentrations from 1.2 nM to 3.6 nM. Interestingly, no NF-Y-mediated DNA looping was detected. In the range of protein concentration explored, NF-Y simply exhibited a histone-like ability to compact DNA. As previously reported (11), there is evidence that although the CCAAT box is preserved in promoters, outside these regions "there might be a plethora of specialized CCAAT versions" and that "it is possible we are largely underestimating the number of binding sites by focusing on the perfect pentanucleotide". Thus, the compaction we observed gives experimental evidence that indeed NF-Y cannot only bind to the CCAAT box but to a variety of DNA sequences. Since NF-Y is a DNA bender, this "nonspecific" binding leads to a certain level of DNA compaction. This is in agreement with the histone-like nature of this protein, which has been suggested to allow it to replace H2A/H2B in the nucleosomal particle (19).

Above 3.6 nM, NF-Y did not induce further compaction, perhaps indicating that at this concentration the protein saturates DNA. This is reasonable given the large excess of NF-Y over potential nonspecific binding sites on the DNA in the microchamber at this protein concentration. Indeed, assuming that each bound NF-Y molecule "protects" ~20 bp of DNA, each of our DNA tethers would contain 1850 bp/ 20 bp = 92.5 nonspecific sites. This, of course, is an upper limit since the actual number of binding sites is much reduced due to end effects and statistical variation in protein placement on the DNA lattice. Yet, even assuming the concentration of sites to be of the order of 10^{-12} M (two orders of magnitude higher than that of DNA; see Materials and Methods), NF-Y is in vast excess. Fig. 3 shows that at each

concentration of NF-Y shown, the compaction of the DNA molecules was constant. This, together with the observation that it was virtually impossible to wash away the protein even with large volumes of protein-free buffer, suggests that NF-Y does not bind and unbind DNA in thermodynamic equilibrium. This is in agreement with what was already observed for other histone-like proteins (20) that can bind both specifically and nonspecifically. Our experiments show that NF-Y, like histones, can modify the architecture of DNA considerably with obvious consequences for DNA-protein and protein-protein interactions. Moreover, the DNA bending and compaction associated with NF-Y binding could soften the DNA to further bending and twisting, as postulated recently for another histone-like protein (21), and could thus favor the interaction between DNA and other factors or between different DNA-bound regulatory proteins. In so doing, NF-Y may perform what is probably its main function in vivo: facilitating promoter-enhancer communication.

Furthermore, our data indicate that not only the presence of the NF-YA subunit but also the presence of both the Q-rich domains, present on NF-YA and NF-YC, are necessary for compaction. Although the dimer contains histone folds and this core domain has been shown to be necessary for DNA binding in the context of the trimeric complex, it cannot compact it, as shown in Fig. 4. This is inconsistent with the suggestion that the dimer NF-YB/NF-YC acts as a histone particle in binding nonspecifically the DNA and escorting NF-YA to the specific binding site. As mentioned above, the monomers NF-YA and NF-YC contain large domains rich in glutamine residues (Fig. 1 B) and hydrophobic residues that have been shown to activate transcription both in transfections and in vitro experiments (22–25). As shown in Fig. 4, mutants without the Q-rich domain of just NF-YA or of both NF-YA and NF-YC have no effect on the conformation of DNA, in stark contrast with the full-length protein. From this, we conclude that the Q-rich domains play a significant role in DNA compaction by NF-Y. No x-ray structures of Q-rich domains' transcriptional factors have been solved. One reason is that these domains are poorly structured. It should be remembered that in addition to high percentages of Qs, these activation domains contain no or few charged residues, as well as a large proportion of hydrophobic residues (isoleucines and leucines), typically in the 30% range. Thus, they might constitute ''sticky'' ends of transcription factors, able to form higher order structures through simple unstructured interactions with other similarly sticky ends.

The compaction induced by NF-Y did not seem to depend on the presence of the two CCAAT boxes present on the Ea fragment (Fig. 3). The same degree of compaction was observed for DNA molecules with or without these specific binding sites. Thus, the CCAAT boxes do not serve as nucleation sites for the extensive, nonspecific binding that leads to compaction and exhibits anomalously high affinity.

Finally, RFX did not induce compaction, as shown in Fig. 5, and even inhibited the compaction induced by NF-Y. We know that RFX binding to the X box is quite unstable, but the presence of NF-Y greatly stabilizes the DNA/RFX/NF-Y nucleoprotein complex (12,16). Comparison of Figs. 3 B and 6 reveals that RFX interferes with NF-Y-induced compaction. Although the difference is small, it is significant, given the precision of the data. The reduced ability of NF-Y to compact DNA in the presence of RFX might indicate a regulatory role for RFX on NF-Y binding to DNA.

Recently, two-hybrid assays suggested that RFX, besides binding cooperatively to DNA in the presence of NF-Y, associates to NF-Y in vivo (26). Furthermore, there is strong evidence that RFX trimers must dimerize to function in vivo (26), and a model has been suggested that implies the formation of an enhanceosome involving NF-Y, a dimer of RFX trimers and CIITA, to activate transcription (27). In such a model the DNA is bent around the NF-Y-RFX dimer complex necessarily with a lower curvature than when it is bent around NF-Y alone. This gentler bending and the increased steric hindrance, due to the larger size of the protein complex, could account for the reduced NF-Y-induced shortening of the DNA in the presence of RFX (Fig. 6). Since we observed that not only does RFX interfere with NF-Y-induced DNA compaction but also the level of such interference seems to increase with increasing NF-Y concentration and consequent DNA compaction, we speculate that RFX may have the role of limiting NF-Y-induced compaction. Indeed, an excessive amount of nonspecific binding of such surprisingly high affinity might cause changes in the DNA architecture that could be deleterious for the cell.

In conclusion, using the TPM technique, we showed that NF-Y, one of the most widespread transcriptional activators in eukaryotic promoters, has a strong, concentration-dependent DNA compaction capability inside the 1.2–3.6 nM range. Such compaction, which is understandable in terms of the DNA bending and histone-like characteristics of NF-Y, may underlie the physiological role of both NF-Y and RFX, a cofactor found in some of the promoters regulated by NF-Y. The DNA compaction induced by NF-Y needs to be kept in check since, if some may facilitate promoter-enhancer communication, excessive levels of it may be toxic (the same is true for many other proteins and enzymes that modify DNA topology, notably topoisomerases). RFX is thus the, or one of the, regulator necessary to control the level of compaction that would be induced by NF-Y alone in DNA. We suggest that this is part of the mechanism by which RFX may contribute to transcriptional activation. Although additional experiments might clarify the role of RFX, these direct measurements reveal how physicochemical parameters such as protein-protein interactions and protein concentrations may affect the conformation of DNA. Such information is useful to model the modus operandi of many regulators in vivo and inspire further experimentation at the cellular level.

REFERENCES

1. Benoist, C., and D. Mathis. 1990. Regulation of major histocompatibility complex class-II genes: X, Y and other letters of the alphabet. *Annu. Rev. Immunol.* 8:681–715.

2. Mantovani, R. 1999. The molecular biology of the CCAAT-binding factor NF-Y. *Gene.* 239:15–27.

3. Suzuki, Y., T. Tsunoda, J. Sese, H. Taira, J. Mizushima-Sugano, H. Hata, T. Ota, T. Isogai, T. Tanaka, Y. Nakamura, A. Suyama, Y. Sakaki, S. Morishita, K. Okubo, and S. Sugano. 2001. Identification and characterization of the potential promoter regions of 1031 kinds of human genes. *Genome Res.* 11:677–684.

4. Sinha, S., I. S. Kim, K. Y. Sohn, B. de Crombrugghe, and S. N. Maity. 1996. Three classes of mutations in the A subunit of the CCAAT-binding factor CBF delineate functional domains involved in the three-step assembly of the CBF-DNA complex. *Mol. Cell. Biol.* 16:328–337.

5. Romier, C., F. Cocchiarella, R. Mantovani, and D. Moras. 2003. The NF-YB/NF-YC structure gives insight into DNA binding and transcriptional regulation by CCAAT factor NF-Y. *J. Biol. Chem.* 278:1336–1345.

6. Mantovani, R., X. Y. Li, U. Pessara, R. Hooft van Huisjduijnem, C. Benoist, and D. Mathis. 1994. Dominant negative analogs of NF-YA. *J. Biol. Chem.* 269:20340–20346.

7. Kim, C. G., and M. Sheffrey. 1990. Physical characterization of CCAAT transcription factor α-CP1. *J. Biol. Chem.* 265:13362–13369.

8. Bi, W., L. Wu, F. Coustry, C. Benoist, B. de Crombrugghe, and S. N. Maity. 1997. DNA binding specificity of the CCAAT-binding factor CBF/NF-Y. *J. Biol. Chem.* 272:26562–26572.

9. Ronchi, A., M. Bellorini, N. Monelli, and R. Mantovani. 1995. CCAAT-box binding protein NF-Y (CBF,CP1) recognizes the minor groove and distorts DNA. *Nucleic Acids Res.* 23:4565–4572.

10. Liberati, C., A. Di Silvio, S. Ottolenghi, and R. Mantovani. 1999. NF-Y binding to twin CCAAT boxes: role of Q-rich domains and histone fold helices. *J. Mol. Biol.* 285:1441–1455.

11. Testa, A., G. Donati, P. Yan, F. Romani, T. H. Huang, M. A. Vigano, and R. Mantovani. 2005. Chromatin immunoprecipitation (ChIP) on chip experiments uncover a widespread distribution of NF-Y binding CCAAT sites outside of core promoters. *J. Biol. Chem.* 280:13606–13615.

12. Reith, W., C. A. Siegrist, B. Durand, E. Barras, and B. Mach. 1994. Function of major histocompatibility complex class II promoters requires cooperative binding between factors RFX and NF-Y. *Proc. Natl. Acad. Sci. USA.* 91:554–558.

13. Finzi, L., and J. Gelles. 1995. Measurement of Lac repressor-mediated loop formation and breakdown in single DNA molecules. *Science.* 267:378–380.

14. Lia, G., D. Bensimon, V. Croquette, J.-F. Allemand, D. Dunlap, D. A. E. Lewis, S. Adhya, and L. Finzi. 2003. Supercoiling and denaturation in GalR/HU-mediated DNA looping as seen by single-molecule microscopy. *Proc. Natl. Acad. Sci. USA.* 100:11373–11377.

15. Koch, W., C. Benoist, and D. Mathis. 1989. Anatomy of a new B-cell-specific enhancer. *Mol. Cell. Biol.* 9:303–311.

16. Caretti, G., F. Cocchiarella, C. Sidoli, J. Villard, M. Peretti, W. Reith, and R. Mantovani. 2000. Dissection of functional NF-Y-RFX cooperative interactions on the MHC class II Ea promoter. *J. Mol. Biol.* 302:539–552.

17. Finzi, L., and D. Dunlap. 2003. Single molecules study of DNA architectural changes induced by regulatory proteins. *Methods in Enzimology.* 370:369–378.

18. Nelson, P., C. Zurla, D. Brogioli, J. F. Beausang, L. Finzi, and D. Dunlap. 2006. Tethered particle motion as a diagnostic of DNA tether length. *J. Phys. Chem. B.* 110:17260–17267.

19. Van Nort, J., S. Verbrugge, N. Goosen, C. Dekker, and R. T. Dame. 2004. Dual architectural roles of HU: formation of flexible hinges and rigid filaments. *Proc. Natl. Acad. Sci. USA.* 101:6969–6974.

20. Ramreddy, T., S. Sen, B. J. Rao, and G. Krishnamoorthy. 2003. DNA dynamics in RecA-DNA filaments: ATP hydrolysis-related flexibility in DNA. *Biochemistry.* 42:12085–12094.

21. Linhoff, W. M., L. K. Wright, and J. P.-Y. Ting. 1997. CCAAT—binding factor NF-Y and RFX are required for in vivo assembly of a nucleoprotein complex that span 250 base pairs: the invariant chain promoter as a model. *Mol. Cell. Biol.* 17:4589–4596.

22. Masternak, K., N. Peyraud, M. Krawczyk, E. Barras, and W. Reith. 2003. Chromatin remodeling and extragenic transcription at the MHC class II locus control region. *Nat. Immunol.* 4:132–137.

23. Schnurr, B., C. Vorgias, and J. Stavans. 2006. Compaction and supercoiling of single, long DNA molecules by HU protein. *Biophys. Rev. Lett.* 1:29–44.

24. Li, X., R. Mantovani, R. Hooft van Huisjduijnem, I. Andre, C. Benoist, and D. Mathis. 1992. Evolutionary variation of the CCAAT-binding transcription factor NF-Y. *Nucleic Acids Res.* 20:1087–1091.

25. Serra, E., K. Zemzoumi, A. di Silvio, R. Mantovani, V. Lardans, and C. Dissous. 1998. Conservation and divergence of NF-Y transcriptional activation function. *Nucleic Acids Res.* 26:3800–3805.

26. Coustry, F., Q. Hu, B. de Crombrugghe, and S. N. Maity. 2001. CBF/NF-Y functions both in nucleosomal disruption and transcription activation of the chromatin-assembled topoisomerase II alpha promoter. Transcription activation by CBF/NF-Y in chromatin is dependent on the promoter structure. *J. Biol. Chem.* 276:40621–40630.

27. Coustry, F., S. Sinha, S. N. Maity, and B. Crombrugghe. 1998. The two activation domains of the CCAAT-binding factor CBF interact with the dTAFII110 component of the Drosophila TFIID complex. *Biochem. J.* 331:291–297.